Characteristics and Mechanism of Bubble Initiation in Transformer Oil Induced by Vibration

Chong Guo[1], Qiaogen Zhang[1], Junjie Zhou[1], Shaoqi Wang[1], Yunhan Sun[1], and Zhetao Zhang[1]

[1]Xi'an Jiaotong University School of Electrical Engineering

April 28, 2023

Abstract

Operating experience has shown that vibration can cause pressure fluctuations and initiate bubbles at the oil gap, which seriously threatens the insulation properties of oil-immersed power equipment. The main aim of this study was to determine the characteristics and mechanism of bubble initiation at the transformer oil gap under vibration in this paper. The results show the existence of the vibration-dependent bubbling phenomenon at the oil gap. Interestingly, bubbles initiate during the process of gap expansion, and the evolution of bubble morphology was further analyzed. The threshold characteristic of the bubble initiation process was found, and the relevant influencing factors were experimentally obtained. In the range considered in this study, higher gas content, higher temperature, and lower moisture content are conducive to bubble initiation at the oil gap under vibration, while vibrational frequency does not affect the threshold characteristic of bubble initiation process. The vibration-dependent bubbling phenomenon can be attributed to the vibration-induced cavitation process caused by the decrease in pressure at the oil gap. The influence mechanism of the above factors on the threshold characteristics of bubble initiation was further discussed. This study contributes to providing a reference for risk assessment of abnormal vibration of oil-immersed power equipment.

Hosted file

`Characteristics and Mechanism of Bubble Initiation in Transformer Oil Induced by Vibration.docx` available at https://authorea.com/users/612224/articles/640255-characteristics-and-mechanism-of-bubble-initiation-in-transformer-oil-induced-by-vibration

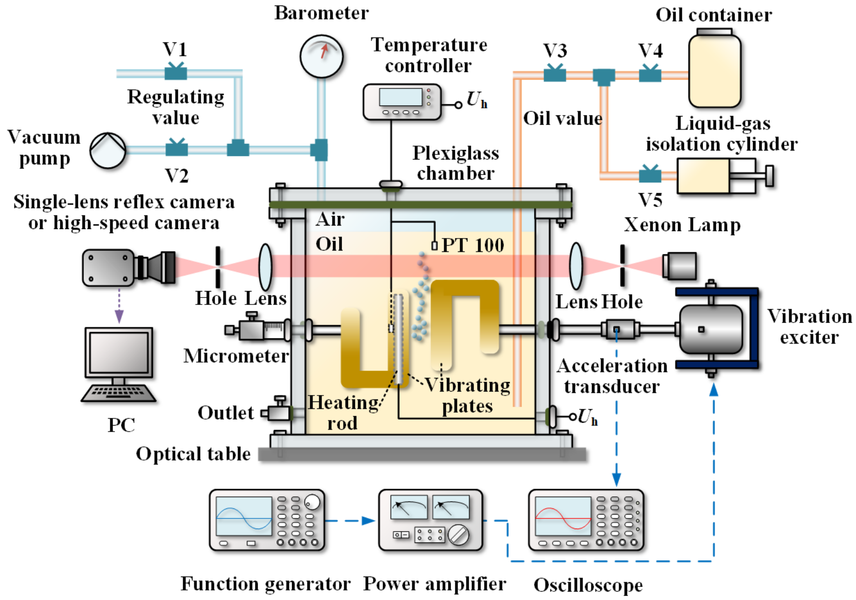
Barometer
Oil container
V1
Temperature controller
V3
V4
U_h
Regulating value
Oil value
Liquid-gas isolation cylinder
Vacuum pump
V2
Plexiglass chamber
V5
Single-lens reflex camera or high-speed camera
Air
Oil
PT 100
Xenon Lamp
Hole
Lens
Lens
Hole
Vibration exciter
Micrometer
Acceleration transducer
Vibrating plates
Outlet
Heating rod
U_h
PC
Optical table
Function generator
Power amplifier
Oscilloscope

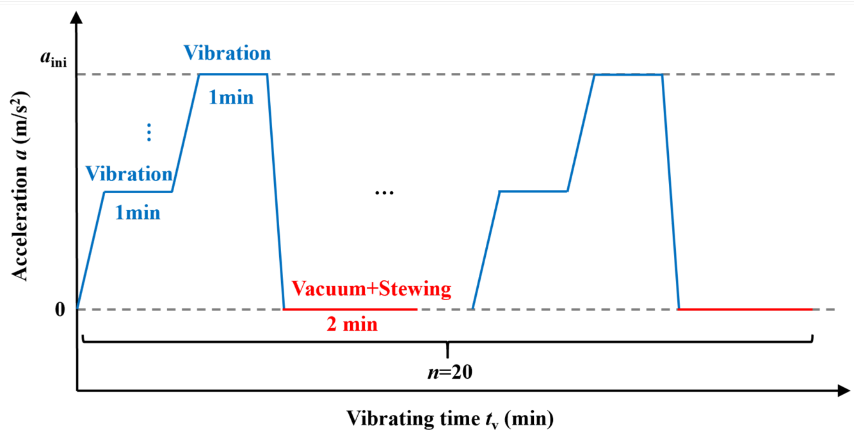
a_{ini}
Vibration
1min
Vibration
1min
...
Vacuum+Stewing
2 min
0
n=20
Acceleration a (m/s^2)
Vibrating time t_v (min)

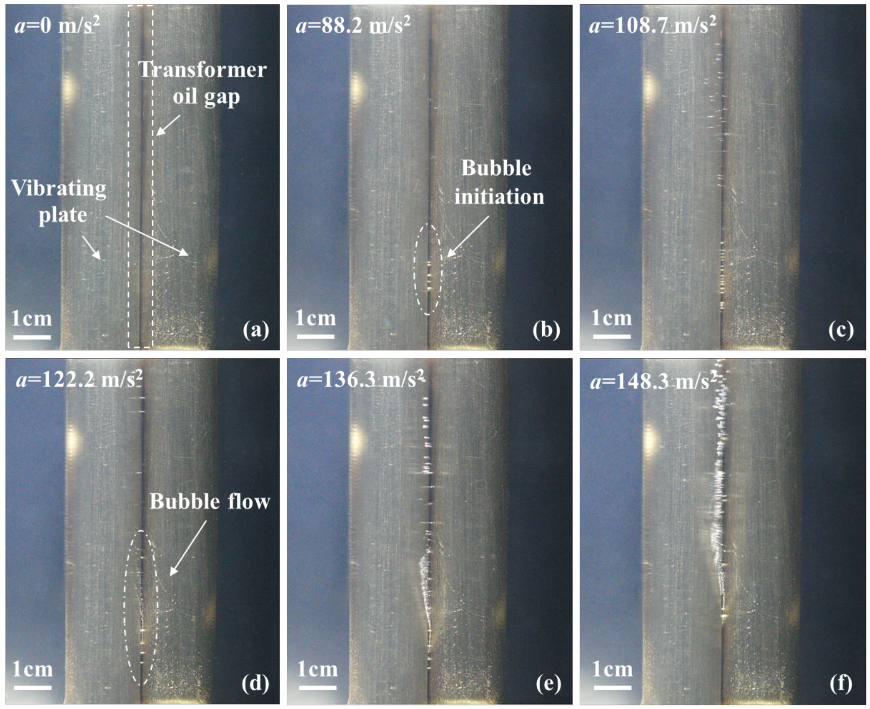

a=0 m/s²
Transformer oil gap
Vibrating plate
1cm
(a)
a=88.2 m/s²
Bubble initiation
1cm
(b)
a=108.7 m/s²
1cm
(c)
a=122.2 m/s²
Bubble flow
1cm
(d)
a=136.3 m/s²
1cm
(e)
a=148.3 m/s²
1cm
(f)

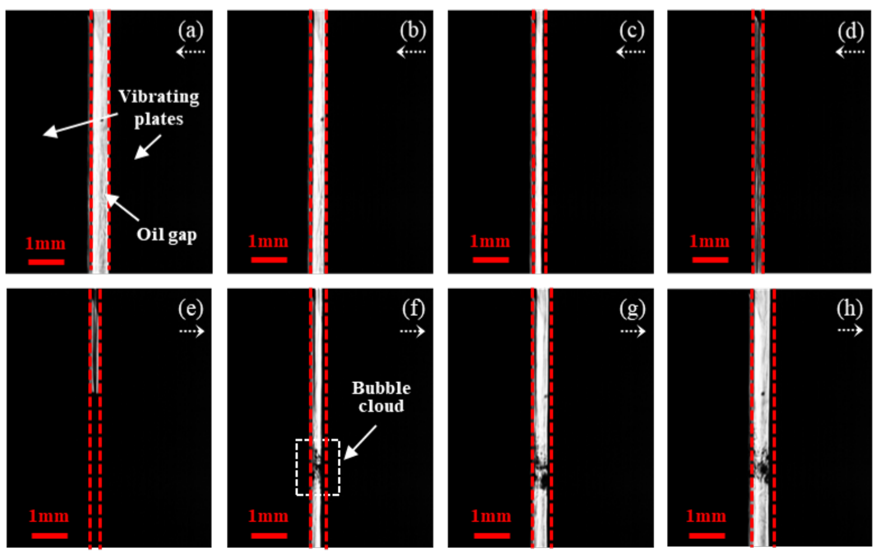

(a)
Vibrating plates
Oil gap
1mm
(b)
1mm
(c)
1mm
(d)
1mm
(e)
1mm
(f)
Bubble cloud
1mm
(g)
1mm
(h)
1mm

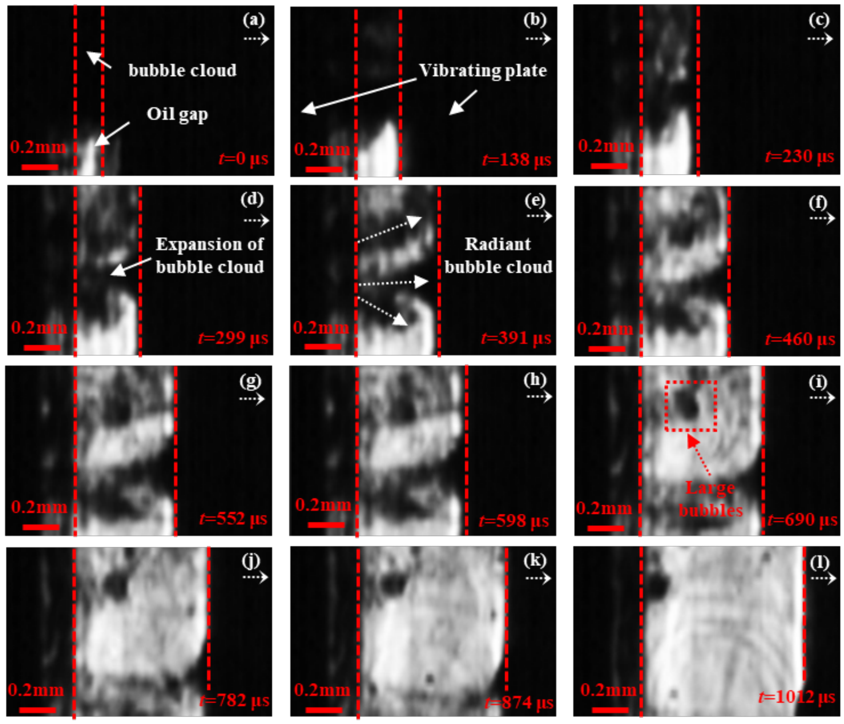

(a)
bubble cloud
Oil gap
0.2mm
t=0 μs
(b)
Vibrating plate
0.2mm
t=138 μs
(c)
0.2mm
t=230 μs
(d)
Expansion of bubble cloud
0.2mm
t=299 μs
(e)
Radiant bubble cloud
0.2mm
t=391 μs
(f)
0.2mm
t=460 μs
(g)
0.2mm
t=552 μs
(h)
0.2mm
t=598 μs
(i)
Large bubbles
0.2mm
t=690 μs
(j)
0.2mm
t=782 μs
(k)
0.2mm
t=874 μs
(l)
0.2mm
t=1012 μs

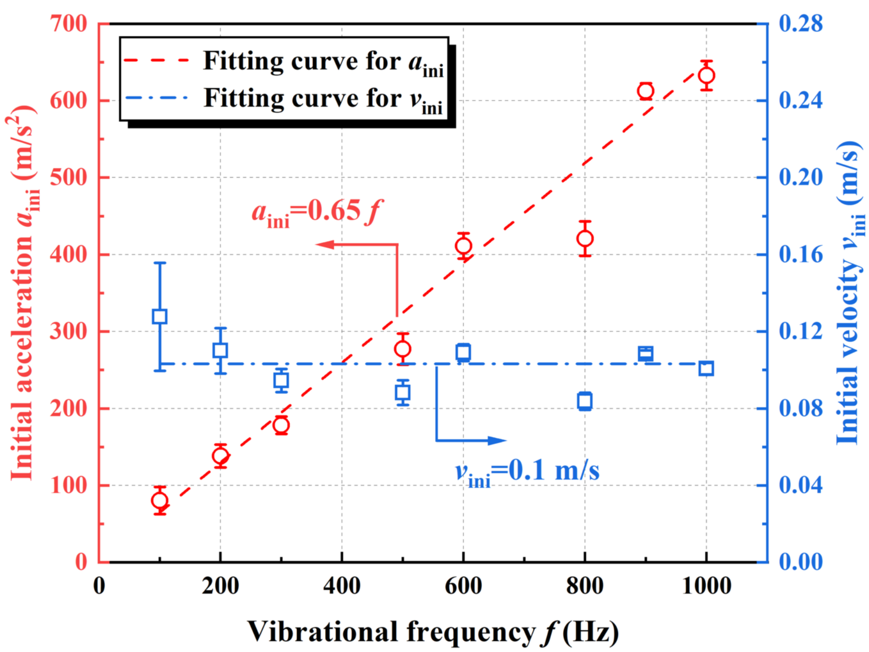

Fitting curve for a_{ini}
Fitting curve for v_{ini}
a_{ini}=0.65 f
v_{ini}=0.1 m/s
Initial acceleration a_{ini} (m/s^2)
Initial velocity v_{ini} (m/s)
Vibrational frequency f (Hz)
0
100
200
300
400
500
600
700
0.00
0.04
0.08
0.12
0.16
0.20
0.24
0.28
0
200
400
600
800
1000

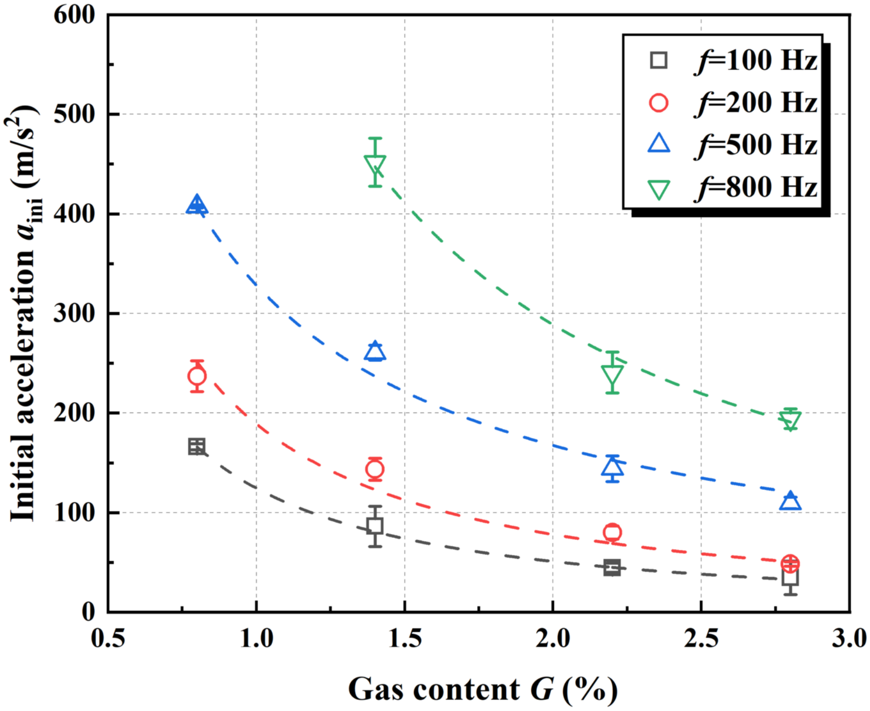

f=100 Hz
f=200 Hz
f=500 Hz
f=800 Hz
Initial acceleration a_{ini} (m/s^2)
Gas content G (%)

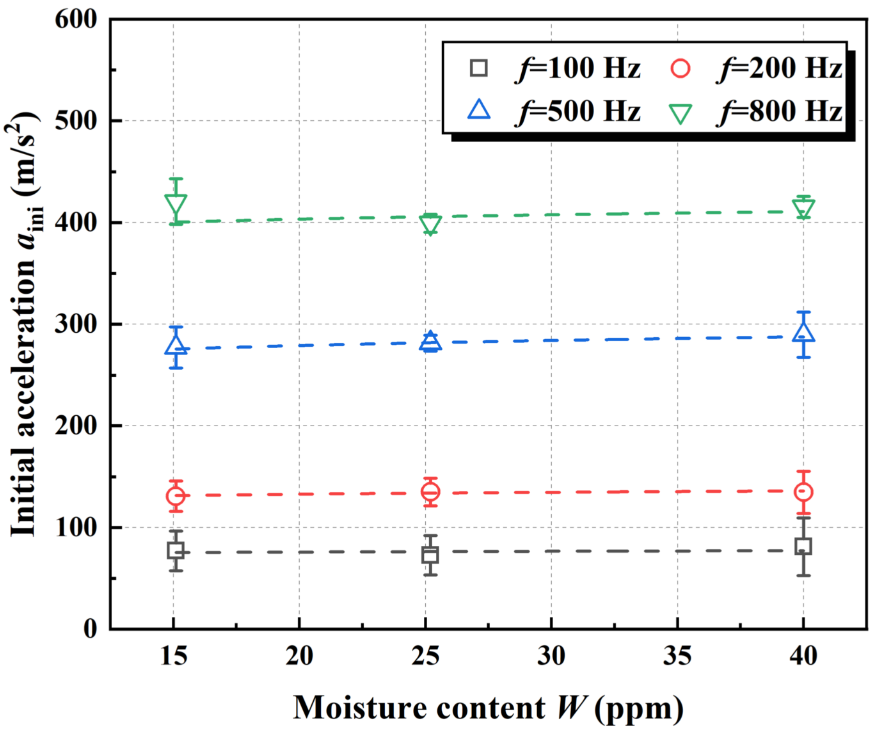

f=100 Hz
f=200 Hz
f=500 Hz
f=800 Hz
Initial acceleration a_{ini} (m/s^2)
Moisture content W (ppm)

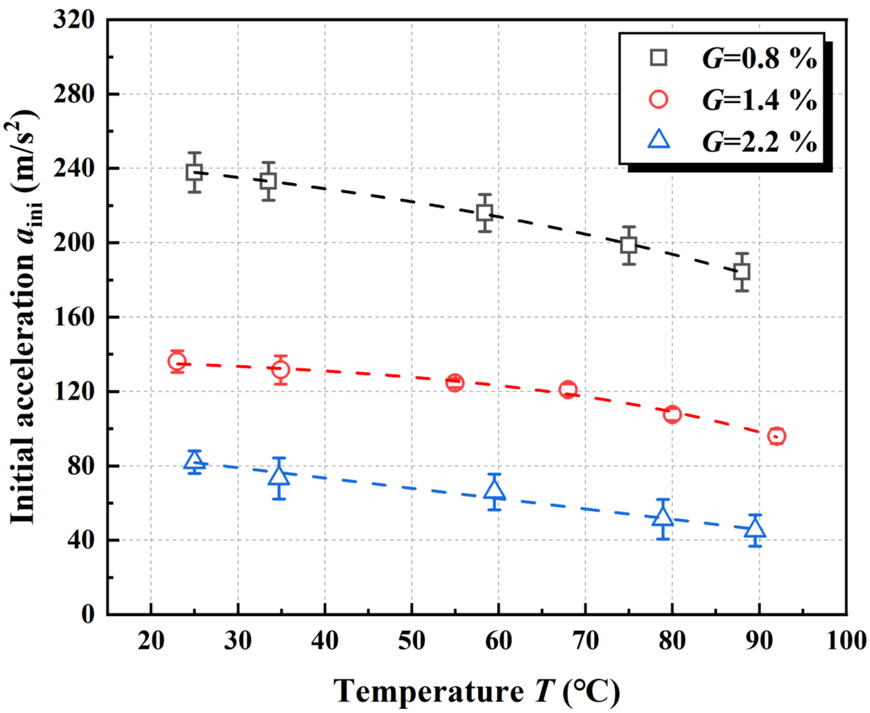
G=0.8 %
G=1.4 %
G=2.2 %
Initial acceleration a_{ini} (m/s^2)
Temperature T (°C)
320
280
240
200
160
120
80
40
0
20
30
40
50
60
70
80
90
100

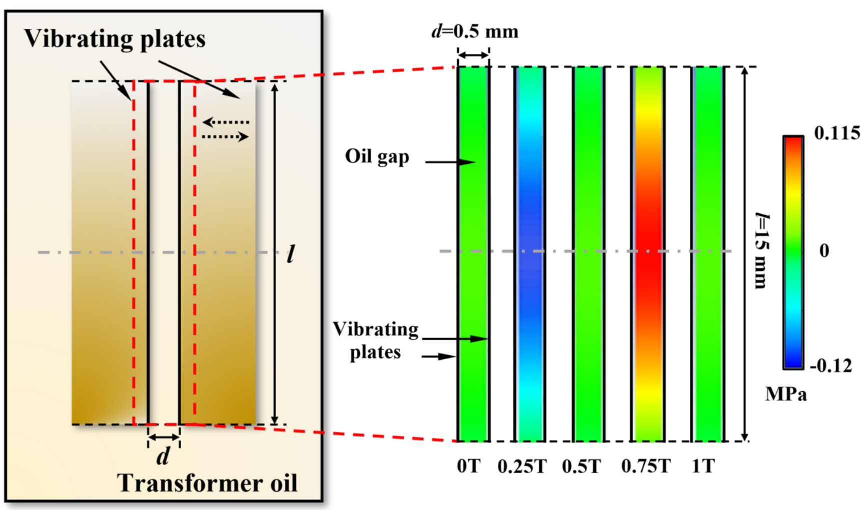
Vibrating plates
l
d
Transformer oil
d=0.5 mm
Oil gap
Vibrating plates
l=15 mm
0.115
0
-0.12
MPa
0T
0.25T
0.5T
0.75T
1T

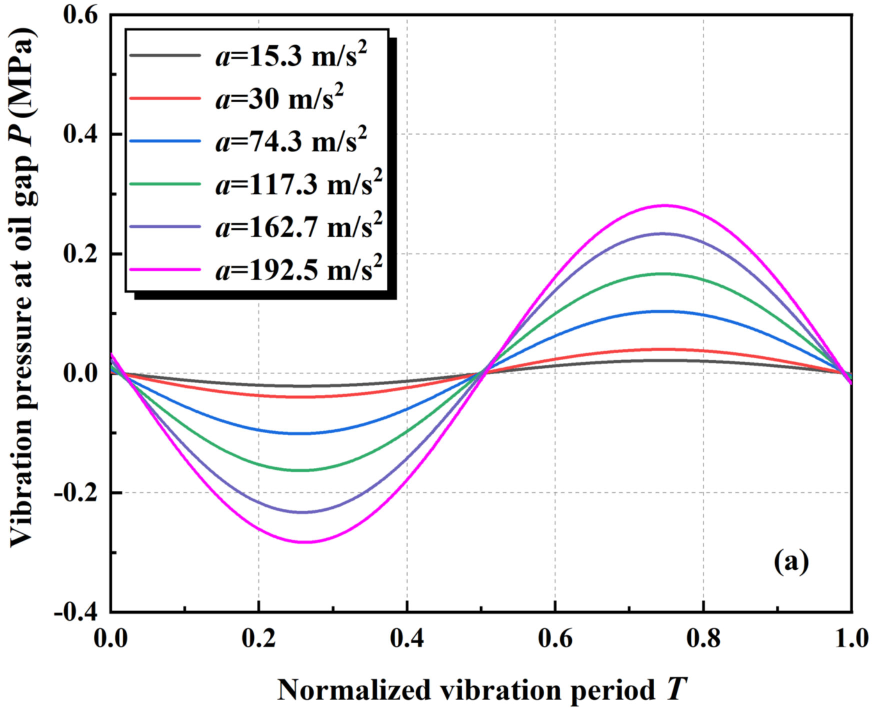

Vibration pressure at oil gap P (MPa)
Normalized vibration period T
a=15.3 m/s2
a=30 m/s2
a=74.3 m/s2
a=117.3 m/s2
a=162.7 m/s2
a=192.5 m/s2
(a)
0.6
0.4
0.2
0.0
-0.2
-0.4
0.0
0.2
0.4
0.6
0.8
1.0

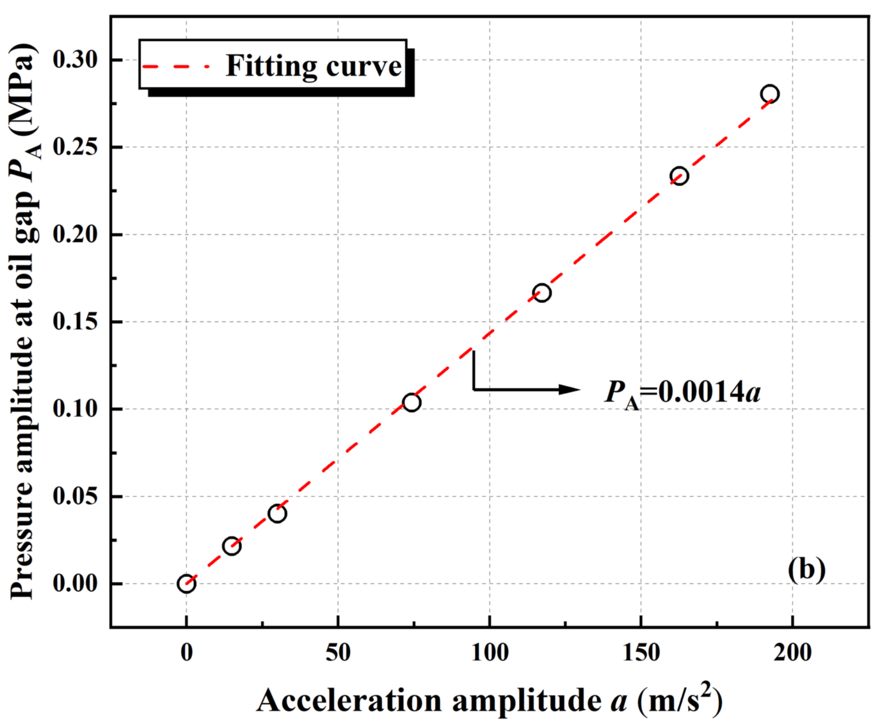

Pressure amplitude at oil gap PA (MPa)
Acceleration amplitude a (m/s2)
Fitting curve
PA=0.0014a
(b)
0.30
0.25
0.20
0.15
0.10
0.05
0.00
0
50
100
150
200

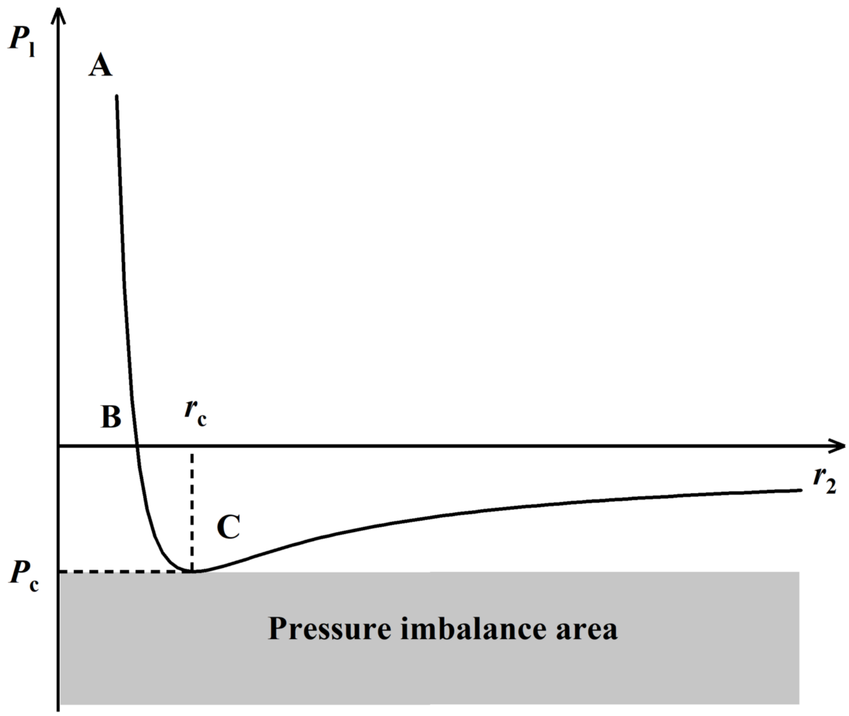

P_1
A
B
r_c
C
r_2
P_c
Pressure imbalance area

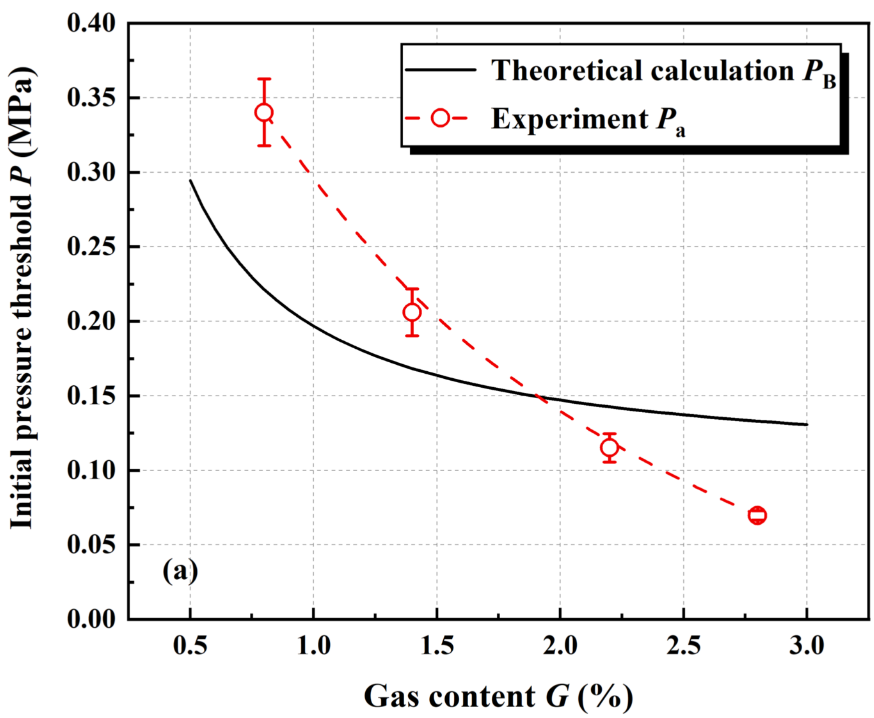

Theoretical calculation P_B
Experiment P_a
Initial pressure threshold P (MPa)
Gas content G (%)
(a)
0.00
0.05
0.10
0.15
0.20
0.25
0.30
0.35
0.40
0.5
1.0
1.5
2.0
2.5
3.0

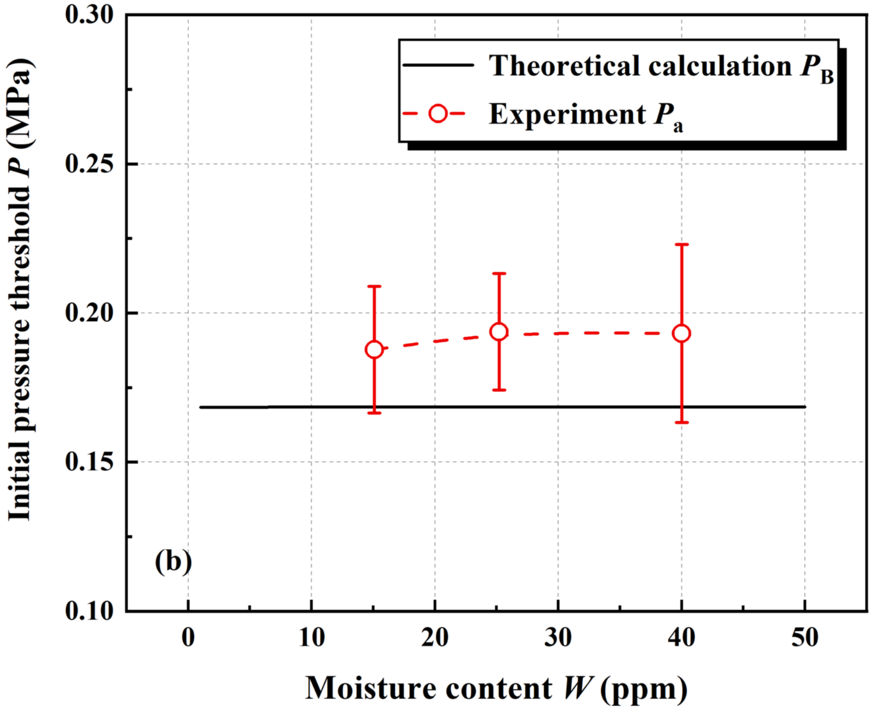

Initial pressure threshold P (MPa)
Moisture content W (ppm)
Theoretical calculation P_B
Experiment P_a
(b)
0.30
0.25
0.20
0.15
0.10
0
10
20
30
40
50

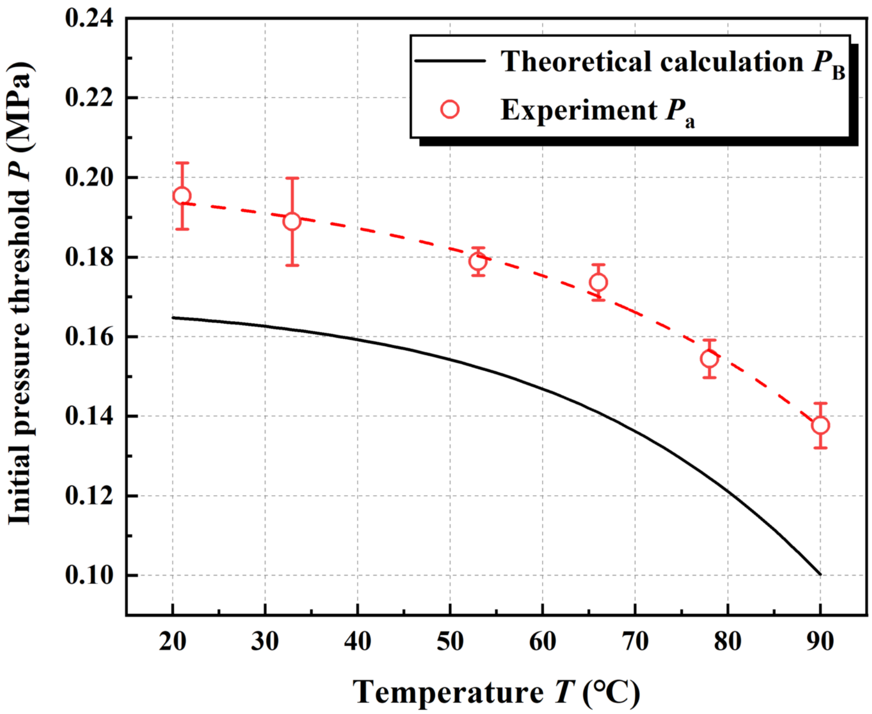

Initial pressure threshold P (MPa)
Temperature T (℃)
Theoretical calculation P_B
Experiment P_a
0.24
0.22
0.20
0.18
0.16
0.14
0.12
0.10
20
30
40
50
60
70
80
90

Characteristics and Mechanism of Bubble Initiation in Transformer Oil Induced by Vibration

All the authors' complete names

Chong Guo

Qiaogen Zhang (correspondence)

Junjie Zhou

Shaoqi Wang

Yuhan Sun

Zhetao Zhang

Departmental & institutional affiliations of the authors

State Key Laboratory of Electric Insulation and Power Equipment
Xi’an Jiaotong University
Xi, an, 710049, P. R. China

Postal & e-mail address of the corresponding author

Email: 835233405@qq.com

Conflict of interest statement

The authors have no conflict whether in the research field or to publish the paper “Characteristics and Mechanism of Bubble Initiation in Transformer Oil Induced by Vibration” on “IET Generation, Transmission & Distribution”.

Funding information

This study was financially supported by the Technology Project of State Grid Anhui Electric Power Company (contract number: 52120520001A).

Data availability statement

The data that support the findings of this study are available from the corresponding author upon reasonable request.

Characteristics and Mechanism of Bubble Initiation in Transformer Oil Induced by Vibration

Chong Guo, Qiaogen Zhang, Junjie Zhou, Shaoqi Wang, Yuhan Sun and Zhetao Zhang
State Key Laboratory of Electric Insulation and Power Equipment
Xi'an Jiaotong University
Xi, an, 710049, P. R. China

ABSTRACT

Operating experience has shown that vibration can cause pressure fluctuations and initiate bubbles at the oil gap, which seriously threatens the insulation properties of oil-immersed power equipment. The main aim of this study was to determine the characteristics and mechanism of bubble initiation at the transformer oil gap under vibration in this paper. The results show the existence of the vibration-dependent bubbling phenomenon at the oil gap. Interestingly, bubbles initiate during the process of gap expansion, and the evolution of bubble morphology was further analyzed. The threshold characteristic of the bubble initiation process was found, and the relevant influencing factors were experimentally obtained. In the range considered in this study, higher gas content, higher temperature, and lower moisture content are conducive to bubble initiation at the oil gap under vibration, while vibrational frequency does not affect the threshold characteristic of bubble initiation process. The vibration-dependent bubbling phenomenon can be attributed to the vibration-induced cavitation process caused by the decrease in pressure at the oil gap. The influence mechanism of the above factors on the threshold characteristics of bubble initiation was further discussed. This study contributes to providing a reference for risk assessment of abnormal vibration of oil-immersed power equipment.

1 INTRODUCTION

Oil-paper insulation systems used in oil-immersed power transformers and high-voltage reactors are inevitably in vibration. The appearance of conditions, such as short-circuit faults, higher harmonics, DC magnetic bias, etc., can intensify the vibration of the core and winding, which is characterized by higher vibration intensity [1-3]. Several bubble-induced oil-paper insulation discharge faults related to abnormal vibration of oil-immersed power equipment have been reported in recent years[4-6]. The reason for the bubble initiation is yet known in this case. Therefore, the conditions and reason for bubble initiation under vibration must be carefully investigated.

There is a large amount of narrow transformer oil gaps in oil-immersed power transformers and high-voltage reactors [7]. As an engineering liquid medium, transformer oil contains a lot of tiny bubble nuclei [8]. Once the bubble nuclei grow to a larger size, it is easy to discharge at a lower electric field intensity, which can significantly reduce the insulation properties of oil-immersed power equipment [9, 10]. Therefore, any possible cause of bubble initiation should be focused on. However, as one of the important causes of bubble initiation, pressure change at the oil gap caused by vibration is often ignored. The vibration can form periodic pressure waves at the transformer oil gap, which become the local pressure lower than the ambient pressure [11,12]. The bubble nuclei are expanded, resulting in the initiation of macroscopic bubbles. That is, the cavitation process caused by vibration appears in transformer oil [13].

Scholars have investigated bubbles initiated under vibration in transformer oil. Heinrichs found that microbubbles intermittently appeared in transformer oil when experimental devices vibrate [14]. Subsequently, Korobeynikov et al explored the bubbling phenomenon with a vibrational frequency of 100 Hz in degassed oil; they found that bubbles initiated in the narrow gaps, and the vibrational cavitation process was considered to be the cause of bubble initiation [15,16]. However, the condition of bubble initiation at the transformer oil gap under vibration is still not clear. There seems to be a lack of research on the mechanism of bubble initiation under vibration as well. Considering the complex and variable operating conditions of oil-immersed power transformers and high-voltage reactors [17,18], the characteristics of bubble initiation may differ depending on factors, such as vibrational frequency, gas content, moisture contents, and temperature of the oil. And how these factors affect the characteristics of bubble initiation at the oil gap under vibration is the question to be answered.

In this paper, the experimental platform, sample preparation, and experimental method are described in section 2. In section 3, the bubbling phenomenon at the transformer oil gap with different accelerations is observed. The threshold characteristics of vibration-induced bubble initiation with different conditions are determined experimentally. Finally, the mechanism of bubble initiation is discussed, combined with the pressure distribution at the oil gap under vibration. The effects of various factors, including vibrational frequency, gas content, moisture content, and temperature of transformer oil, on the threshold characteristics of the bubble initiation process are further analyzed. The results presented in this paper may provide theoretical support for the bubble initiation suppression method of oil-immersed power transformers and high-voltage reactors under abnormal vibration.

2 EXPERIMENTAL SETUP

2.1 EXPERIMENTAL PREPARATION

The experimental platform was composed of four parts: a test chamber with a fluid circuit, a vibration simulation and measurement system, a temperature control system, and a bubble shadow imaging system, as schematically shown in Figure 1. The test chamber was a 100×150×200 mm^3 plexiglass container filled with transformer oil, fixed on an optical table. Two U-shaped copper vibrating plates with a gap distance (d) of 0.5 mm were placed vertically parallel to each other in the center of the chamber. The surface of the vibrating plates was well polished and the effective length of the vibrating plates (l) was 15 mm. The left vibrating plate was connected to the micrometer to accurately adjust the gap distance, and the right vibration plate was connected to the exciter to generate periodic vibration. A liquid-gas isolation cylinder was set horizontally to keep the balance of pressure in and out of the chamber. The treated oil samples from the oil container were injected into the chamber by adjusting the vacuum pump and valves.

We used a vibration exciter to form a sinusoidal vibration in the oil gap. The vibration exciter (1000 m/s^2, 5 Hz~6 kHz) was driven by a vibration simulation and measurement system, which includes the function generator, power amplifier, oscilloscope, and acceleration transducer. A sinusoidal voltage waveform with different frequencies was generated via a function generator (Tektronix® AFG3022C, 0.2 Hz~25 MHz) and was then amplified by a power amplifier. By adjusting the driving power of the power amplifier, the amplitude of acceleration was continuously adjusted. The right vibration plate was rigidly connected to the acceleration transducer and exciter through a dynamic sealing structure in sequence. The vibrational frequency (f) and acceleration (a) were monitored in real-time through the oscilloscope (Tektronix® MDO3012, 100 MHz, 2.5 Gs/s).

A heating rod (250W/220 V_{rms}) was embedded in the left vibrating plate to heat the chamber. The heating power was adjusted by varying the voltage at the heating rod ports (U_h), which in turn controlled the heating temperature (T). The temperature inside the test chamber was recorded in real-time using a temperature controller and PT 100.

The shadow imaging system included a lens group, a Xenon lamp (Zolix®, GLORIA-500A), two holes, and a high-speed frame camera (Motion Pro, 1000 fps), which was employed to capture time-resolved images of the bubble initiation process at the oil gap under vibration. A single-lens reflex camera (Nikon D300) was used to record the vibration-dependent bubbling phenomenon with long exposures.

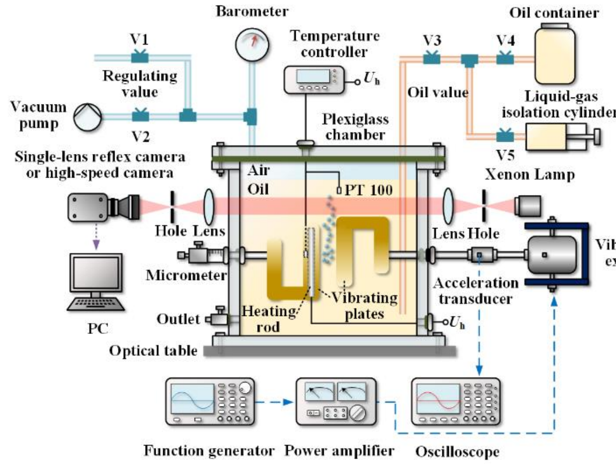

FIGURE 1 Schematic diagram of experimental platform.

2.2 SAMPLE PREPARATION

Before the experiment, Kunlun KI50X transformer oil was preprocessed by drying and degassing in a vacuum drying oven at 75 ℃ and 1 kPa for 48 h to meet the standard IEC 60641-2007 [19]. After drying, the treated oil was placed in a sealed oil container and left to stand for 24 h before subsequent experimentation. Subsequently, oil samples with moisture contents (W) of 14.9 ppm, 25.2 ppm, and 40 ppm were prepared in a constant temperature and humidity chamber, and the moisture content was tested using Karl Fischer titration. In addition, oil samples with gas contents of 0.8%, 1.4%, 2.2%, and 2.8% were prepared in a vacuum drying oven with different processing times, and gas contents were tested using the gas chromatograph (Shanghai Huaai Chromatograph Ltd, GC-9560-HD).

2.3 EXPERIMENTAL METHOD

Acceleration is considered to be the main parameter to characterize the vibration characteristics of oil-immersed power transformers and high-voltage reactors. Thus, we used acceleration to characterize vibration intensity at the oil gap. The initial acceleration of bubbles (a_{ini}) at the oil gap was obtained by increasing the acceleration step by step, as shown in Figure 2. Each vibration lasted for 1 min until continuous bubbles were observed at the oil gap. The output characteristics of the exciter and the sensitivity of the acceleration sensor were considered to determine the acceleration rise rate ($\Delta a/\Delta t$) is 5 m/s^2 per minute. After each experiment, the samples were vacuumed and left to stand for 1 min in sequence to remove any remaining bubbles. The final value reported here was the average of twenty measurements. All the experiments were carried out at ambient pressure.

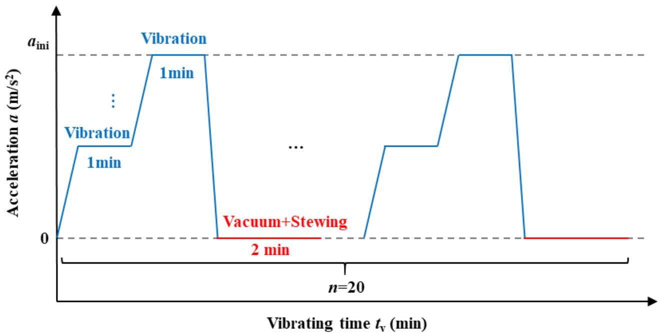

FIGURE 2 Schematic diagram of experimental method. a_{ini} is the initial acceleration of bubbles at the oil gap. n is the number of replicates for each experiment.

3 RESULTS

In this section, experimental studies on the vibration-dependent bubbling phenomenon and the evolution of bubble morphology at the transformer oil gap were carried out, which could help us to better understand the mechanism of bubble initiation. Furthermore, the effects of vibrational frequency, gas content, moisture content, and temperature of oil on threshold characteristics of bubble initiation under vibration were determined experimentally.

3.1 VIBRATION-DEPENDENT BUBBLING PHENOMENON AT TRANSFORMER OIL GAP

The bubbling phenomenon at the transformer oil gap with different accelerations was recorded by a single-lens reflex camera, as shown in Figure 3. No bubbles were observed when acceleration (a) was relatively small. It was found that the bubble initiation at the oil gap when a increased to 88.2 m/s^2. The particle size of a bubble was tens of micrometers, and the initial rate of the bubble was relatively low (Figure 3b). The number and initial rate of the bubble increased with the increase of a (Figure 3c). A bubble flow structure composed of rapidly

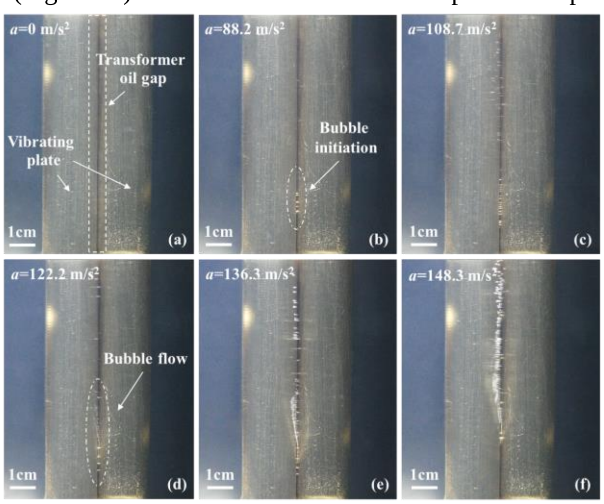

FIGURE 3 Vibration-dependent bubbling phenomenon at transformer oil gap during acceleration increase. Exposure time: 30 ms, vibrational frequency: 200 Hz, gas content: 1.68%, moisture content: 12 ppm, temperature: 23 °C.

migrating bubbles could be observed near the gap when a increased to 122.2 m/s^2 (Figure 3d). As a further increase, it could be observed that a significant increase in bubble flow density and the bubble rising speed (Figure 3e and 3f). The results indicate that bubbles can appear in the transformer oil gap under vibration. When the acceleration exceeded a certain critical value, bubbles appear in the transformer oil gap, and the bubbling phenomenon is enhanced with the increase in acceleration.

Considering the small gap distance and the fast migration rate of bubbles, the shadow imaging system was used to further observe the initiation and morphological evolution process of bubbles at the oil gap. A gap distance (d) of 1 mm and an acceleration (a) of 281.3 m/s^2 were chosen for observation purposes. The initial position of the right vibrating plate was 0.5 mm from the left vibrating plate. The bubble initiation process was captured in a 1/4 vibration period, as shown in Figure 4. The dashed arrows indicate the direction of motion of the vibrating plate. It can be found that bubbles initiate during the expansion of the oil gap and exist in the form of bubble clouds (Figure 4e-4h). Vibration may change the pressure distribution in the oil gap and thus affect the bubble initiation process, which is discussed in detail in the next section.

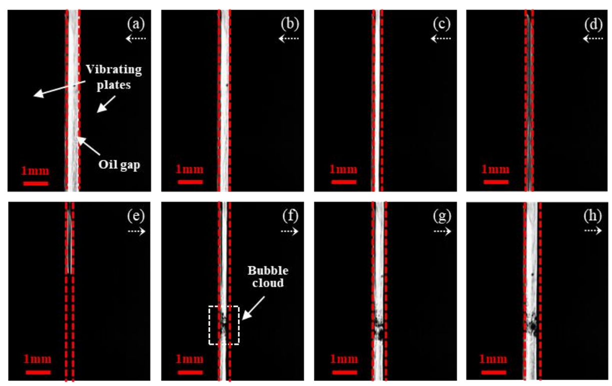

FIGURE 4 Shadow images of the bubble initiation process at the oil gap under vibration. The dashed arrows indicate the direction of motion of the vibrating plate. Exposure time: 250 μs, acceleration: 281.3 m/s^2, vibrational frequency: 200 Hz, gas content: 1.68%, moisture content: 12 ppm, temperature: 23 °C.

To further investigate the evolution of bubble morphology during oil gap expansion, the bubble initiation region in Figure 4 was observed with shorter exposure time of 23 μs, as shown in Figure 5. It appears that the bubble cloud initiated from the surface of the left vibrating plate and radiated radially to the surrounding transformer oil (Figure 5e). As the oil gap expanded, the volume of the bubble cloud gradually increased and large bubbles appeared (Figure 5f). A portion of bubbles can escape from the gap with the oil flow and form the bubble flow shown in Figure 3 during the subsequent gap compression process.

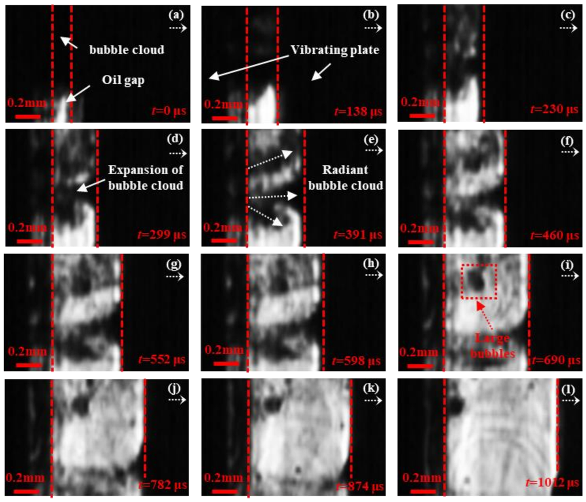

FIGURE 5 Shadow images of the bubble initiation process at the oil gap under vibration. The dashed arrows indicate the direction of motion of the vibrating plate. Exposure time: 250 μs, acceleration: 281.3 m/s^2, vibrational frequency: 200 Hz, gas content: 1.68%, moisture content: 12 ppm, temperature: 23 °C.

In summary, there was a significant bubbling phenomenon at the oil gap under vibration. The process of bubble initiation and morphological evolution was observed as well. In addition, the vibration-dependent bubbling phenomenon at the oil gap has significant threshold characteristics.

3.2 THRESHOLD CHARACTERISTICS OF BUBBLE INITIATION UNDER VIBRATION

There is a risk of bubble initiation at the oil gap under vibration [15,16]. Therefore, it is of great significance to clarify the initial conditions of bubbles at the oil gap under vibration. The main vibrational frequency of oil-immersed power transformers and high-voltage reactors is concentrated between 100 Hz and 500 Hz, and the acceleration with frequencies above 1 kHz is relatively small [20-21]. Considering that the initial acceleration of bubbles (a_{ini}) may vary with different vibrational frequencies, the relationship between a_{ini} and f was first experimentally obtained, as shown in Figure 6. It can be seen that a significantly increased with the increase of f in the case.

The process of bubble initiation under vibration is closely related to the pressure in oil. Due to the small gap distance, it can be assumed that a plane pressure wave is formed. According to the plane pressure wave radiation theory, the spatiotemporal dependence of pressure at the gap (P) and velocity of the vibrating plate (v) are identical and there is no phase difference. The relationship between v and P is as follows [11, 12]:

$$v(x,t)=\frac{1}{\rho c}P(x,t) \tag{1}$$

where ρ is the density of transformer oil; c is the velocity of sound in transformer oil. The pressure amplitude at the gap is determined by the velocity amplitude of the vibrating plate. Without considering the phase, when f is constant, the numerical relationship between v and a of the vibrating plate can be expressed as:

$$v=\frac{a}{\omega}=\frac{a}{2\pi f} \tag{2}$$

Acceleration is widely regarded as a directly measured parameter that characterizes the vibration characteristics of the equipment [1-3, 20, 21]. Therefore, acceleration was still chosen to characterize the vibration intensity of the vibrating plate in this paper. It is reasonable to use a to characterize the difficulty of bubble initiation at the gap with the same f. However, v is necessary to be used to characterize the difficulty of bubble initiation when f changes. As shown in Figure 6, there was no significant change in the initial velocity threshold of bubbles (v_{ini}) with different f. The results indicate that vibrational frequency hardly affects the threshold characteristics of bubble initiation at the oil gap.

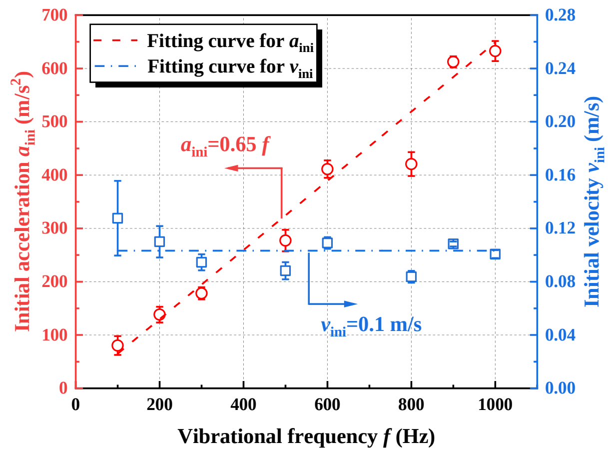

FIGURE 6 Initial acceleration and initial velocity of bubbles at the oil gap with different vibrational frequencies. Gas content: 1.4%, moisture content: 14.9 ppm, temperature: 25 °C.

The gas content in transformer oil will increase due to the aging of oil-paper insulation and equipment maintenance [22]. It is easy for bubble initiation at the oil gap under vibration. Figure. 7 shows the initial acceleration of bubbles (a_{ini}) at the oil gap with different gas contents (G). It appears that a_{ini} gradually decreases with the increase of G with different f, indicating that the increase in gas content promotes bubble initiation at the oil gap under vibration. As an engineering liquid

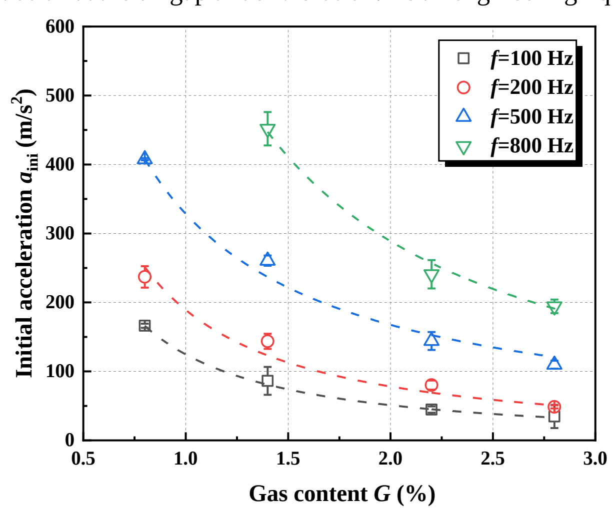

FIGURE 7 The initial acceleration of bubbles at the oil gap with different gas contents. f is vibrational frequency. Moisture content: 14.9 ppm, temperature: 25 °C.

medium, transformer oil inevitably has a large number of bubble nuclei. The radius and number of bubble nuclei in the oil increase with the increase in gas content, which may affect the initial acceleration of bubbles at the oil gap under vibration.

Moisture gradually accumulates in oil-paper insulation as equipment ages [23]. Moisture content is one of the important parameters to characterize the insulation properties of transformer oil. Figure. 8 shows the initial acceleration of bubbles (a_{ini}) at the oil gap with different moisture content (W). Overall, a_{ini} increased slightly with the increase of W under different f. The results indicate that the increase in moisture content has a weak inhibitory effect on the bubble initiation process at the oil gap under vibration. The change in moisture content can affect the surface tension coefficient of transformer oil (σ), and the latter can change the additional pressure by surface tension, which may affect the initial acceleration of bubbles.

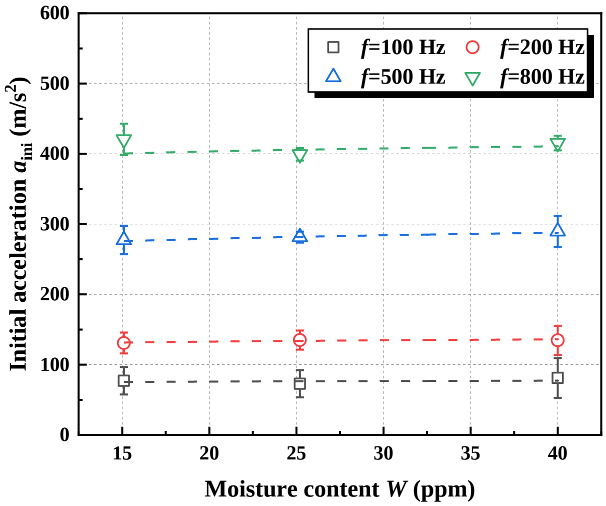

FIGURE 8 The initial acceleration of bubbles at the oil gap with different moisture content. f is vibrational frequency. Gas content: 1.4%, temperature: 25 ℃.

The temperature of transformer oil varies with the load rate of the equipment, which can affect the vapor pressure in the bubble nuclei [24, 25]. The relationship between the initial acceleration of bubbles (a_{ini}) and temperature (T) was experimentally obtained, as shown in Figure 9. As T increased, a_{ini} gradually decreased, indicating that it is easier to initiate bubbles at the oil gap with high temperatures. The variation trend of the a_{ini}-T curves was consistent with different G. As G increased, the curve moved in the direction of decreasing a_{ini}. It indicates that higher temperature and gas content significantly reduce the initial acceleration of bubbles at the oil gap under vibration.

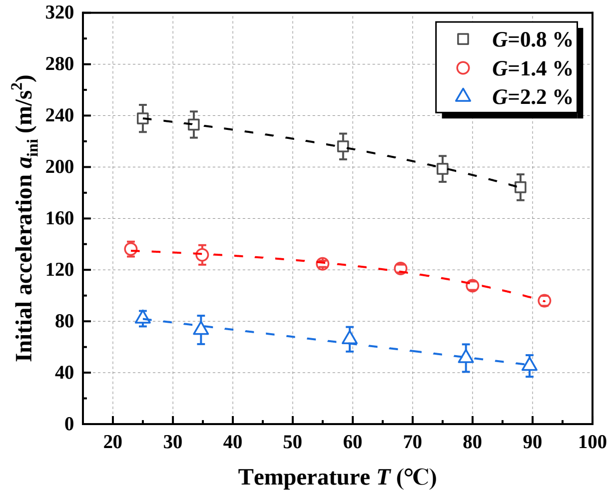

FIGURE 9 The initial acceleration of bubbles at the oil gap with different oil temperatures. G is the gas content of transformer oil. Moisture content: 14.9 ppm.

In summary, the threshold characteristics of bubble initiation at the oil gap under vibration vary with different conditions. In the range considered in this study, higher gas content, higher temperature, and lower moisture content are conducive to bubble initiation at the oil gap under vibration, while vibrational frequency does not affect the threshold characteristics of the bubble initiation process.

4 DISCUSSION

In this section, the bubbling phenomenon and the acceleration threshold for bubble initiation with different conditions have been experimentally obtained from previous studies. In this section, the pressure distribution at the oil gap under vibration was obtained. The mechanism of bubble initiation at the oil gap was further analyzed in combination with the vibration-induced cavitation process.

4.1 PRESSURE DISTRIBUTION AT OIL GAP UNDER VIBRATION

The bubbling phenomenon and the threshold characteristics of bubble initiation under vibration are determined by the pressure at the oil gap, and the latter is closely related to acceleration. Therefore, it is necessary to clarify the relationship between acceleration (a) and vibration pressure (P). The vibration pressure distribution at the oil gap was calculated by the computational fluid dynamics (CFD) method based on fluid dynamics calculation software. As an example, a relative pressure distribution nephogram within one vibration period was depicted in Figure 10. The acceleration is 74.3 m/s^2 and the vibrational frequency is 200 Hz. It can be seen that the pressure in the middle of the gap decreases rapidly when the gap expands. Therefore, bubbles tend to initiate when the gap expands. In addition, it appears that the pressure change in the center area of the left vibrating plate surface is the most obvious. Bubbles tend to form where the intensity of vibration is greatest at the oil gap [15, 16], so only maximum vibration pressure is discussed.

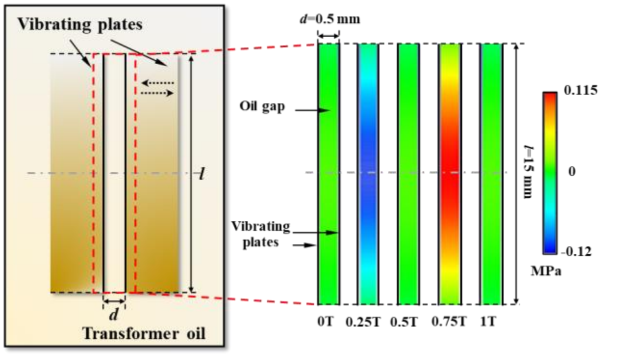

FIGURE 10 Relative pressure distribution nephogram at the oil gap under vibration. *d* is the gap distance. *l* is the effective length of the vibrating plates.

Further, the relationship between vibration pressure and acceleration at the oil gap was obtained, as shown in Figure 11. Note that the pressure at the gap changed sinusoidally (Figure 11a). When the gap expanded and compressed, negative pressure and positive pressure were formed, respectively. That is the rarefaction phase and the compression phase of vibration pressure. With the increase of a, the vibration pressure amplitude gradually increased. Subsequently, the vibration pressure amplitudes (P_A) with different a were shown in Figure 11b and they were linearly correlated. The vibration pressure amplitude at the oil gap under vibration with different accelerations can be approximately obtained in Figure 11b.

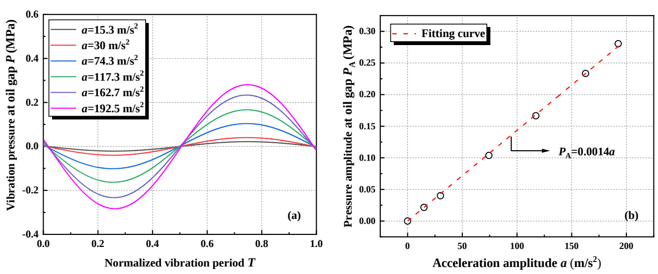

FIGURE 11 Relationship between vibration pressure and acceleration at the oil gap. (a) Time domain waveform of vibration pressure with different acceleration at the central area of the oil gap. (b) Pressure amplitude with different acceleration amplitude.

In summary, the pressure distribution and the relationship between vibration pressure and acceleration at the oil gap under vibration were obtained by the CFD method. The results can serve as the basis for analyzing the mechanism of bubble initiation, which is described in detail in the next section.

4.2 MECHANISM OF BUBBLE INITIATION AT OIL GAP INDUCED BY VIBRATIONAL CAVITATION PROCESS

There are a large number of tiny bubble nuclei in transformer oil. We focus on the mechanism of the transformation of bubble nuclei into macroscopic bubbles under vibration in this section. The total pressure inside and outside the bubble nuclei is the key to determining the bubble initiation process. For a bubble nucleus in transformer oil, its dynamic equilibrium condition without external disturbance can be expressed as:

$$P_g + P_v = P_l + P_\sigma \tag{3}$$

where P_g and P_v are the partial pressure of gases and vapor pressure inside the bubble nucleus, respectively. Air and water vapor are considered to be the main components inside bubble nuclei in oil [6,8]. Thus, P_v can be expressed as water saturation vapor pressure in the constant temperature. P_l is the pressure in oil, P_σ is the additional pressure by surface tension, which can be further expressed as:

$$P_\sigma = \frac{\sigma}{2r} \tag{4}$$

where σ is the surface tension coefficient, r is the radius of the bubble nucleus.

The volume of the bubble nucleus (V) changes with P_l, and then the pressure inside and outside the bubble nucleus reaches a new equilibrium state. To completely determine the state of the bubble nucleus, the initial state and the disturbed state of the bubble can be expressed as:

$$\begin{aligned} P_{g1} + P_{v1} &= P_{l1} + P_{\sigma1} \\ P_{g2} + P_{v2} &= P_{l2} + P_{\sigma2} \end{aligned} \tag{5}$$

where corner symbols "1" and "2" represent the initial state and the disturbed state of the bubble nucleus, respectively.

Considering that the temperature rise rate of transformer oil is generally lower than 15 K/min [24, 25], which is much smaller than the pressure change rate. Therefore, the growth process of bubble nuclei can be approximately regarded as an adiabatic process [11, 12], which can be expressed as:

$$P_{g1} V_1^{\kappa} = P_{g2} V_2^{\kappa} \tag{6}$$

where κ is the adiabatic exponent. For air and water vapor inside the bubble, κ=1.4.

Further, combining Equations (5) and (6), the relationship between P_l and r is as follows:

$$P_{l2} = (P_{l1} + P_{\sigma1} - P_v)\left(\frac{r_1}{r_2}\right)^{3\kappa} + P_v - P_{\sigma2} \tag{7}$$

To analyze the growth process of bubble nuclei at the oil gap under vibration, the schematic diagram of Equation (7) was shown in Figure 12. It can be found that the pressure in oil is composed of positive pressure terms and negative pressure terms. When r_2 is small, P_{l2} is mainly contributed by the positive pressure term. When r_2 is large, the negative pressure term plays an important role in P_{l2}. P_{l2} gradually decreased from point A and r_2 increased under the vibration negative pressure phase. When P_{l2} decreased to point B, the pressure changed from positive to negative. r_2 could reach the critical position C by further reducing P_{l2}. At this point, if the pressure was further reduced, r_2 could no longer satisfy Equation (7). It indicates that the pressure inside the bubble nucleus is higher than the pressure outside. The bubble nucleus begins to expand rapidly and form a macroscopic bubble. That is the vibration-induced cavitation process of the bubble nucleus at the oil gap. Therefore, the vibration-dependent bubble initiation process at the oil gap has significant threshold characteristics.

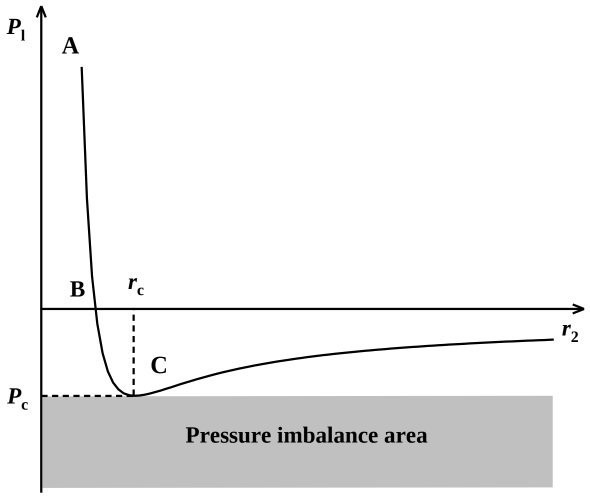

FIGURE 12 Schematic diagram of the relationship between pressure in oil and radius of bubble nucleus. P_c is the critical pressure, r_c is the critical radius.

To quantify the initial condition of bubbles at the oil gap under vibration, the initial pressure threshold is further determined here. The initial state of the bubble nucleus can be considered as the state without disturbance. Therefore, P_{l1} and r in Equation (7) can be represented as environmental pressure (P_0) and the initial radius (r_0) of the bubble nucleus, respectively. By derivative of r_2 in Equation (7), we can obtain the expression of the critical radius r_c:

$$r_c=\left[\frac{3\kappa}{2\sigma}\left(P_0+\frac{2\sigma}{r_0}-P_v\right)r_0^3\right]^{\frac{1}{3\kappa-1}} \tag{8}$$

Combining Equations (7) and (8), the critical pressure (P_c) in oil that leads to the cavitation process of bubble nuclei can be expressed as:

$$P_c=(P_0+\frac{2\sigma}{r_0}-P_v)(\frac{r_0}{r_c})^{3\kappa}+P_v-\frac{2\sigma}{r_c} \tag{9}$$

Further, the initial pressure threshold (P_B) of bubbles at the oil gap under vibration can be expressed as:

$$P_B=P_0-P_c=P_0-(P_0+\frac{2\sigma}{r_0}-P_v)(\frac{r_0}{r_c})^{3\kappa}-P_v+\frac{2\sigma}{r_c} \tag{10}$$

According to the results shown above, P_B is determined by the initial radius of the bubble nucleus (r_0), surface tension coefficient of transformer oil (σ), and water saturation vapor (P_v). Larger bubble nuclei, lower surface tension coefficient, and higher vapor pressure are all conducive to bubble initiation at the oil gap under vibration. And P_B does not change with vibrational frequency (f).

Many previous studies have shown that r_0, σ, and P_v are closely related to the gas content (G), moisture content (W), and temperature (T) of the oil. The relevant research results were used to establish the relationship between r_0, σ, P_v and G, W, T, which can be expressed as [18, 26, 27]:

$$r_0=0.26G^{0.94} \tag{11}$$

$$\sigma=29.1W^{0.0024} \tag{12}$$

$$P_v=4.6\times10^6 exp\left[-\left(\frac{T-590.7}{111.3}\right)^2\right] \tag{13}$$

Based on Equations (10)-(13), the initial pressure threshold (P_B) was calculated with different gas contents, moisture contents, and temperatures of the oil. Meanwhile, to compare with the theoretical calculation results, the initial accelerations (a_{ini}) obtained from the experiment in Figure 7-9 were transformed into the initial pressure (P_a) according to the results in Figure 11b. As shown in Figure 13, the theoretical calculation results are in good agreement with the experimental results in terms of the order of magnitudes and influence laws. The correctness of the mechanism of bubble initiation induced by the vibrational cavitation process is preliminarily verified. Due to the resolution of the observation equipment, there is a certain deviation between the theoretical calculation results (P_B) and the experimental results (P_a). The interaction between bubble nuclei is ignored as well in this paper.

Subsequently, the influence mechanism of gas content, moisture content, and temperature on the threshold characteristics of bubble initiation under vibration was further analyzed. According to Henry's law, the partial pressure in bubble nuclei increases with the increase in gas content. Larger bubble nuclei are more likely to appear in oil in this case. In addition, the number of bubble nuclei also increases with the increase in gas content, leading to a decrease in the initial acceleration and pressure at the oil gap under vibration (Figure 13a).

The surface tension coefficient of oil slightly increases with the increase in water content, and the additional pressure of surface tension also increases, which has an adverse effect on the growth of bubble nuclei. Considering the low increase of surface tension coefficient, moisture content has little effect on the initial acceleration and pressure at the oil gap under vibration (Figure 13b).

Water saturation vapor pressure increases exponentially with the increase in temperature, resulting in a rapid increase in pressure inside bubble nuclei. Only a lower vibration pressure needs to be provided in the oil to induce the vibrational cavitation process of bubble nuclei. Therefore, the initial acceleration and pressure decrease rapidly as temperature increases at the oil gap under vibration (Figure 13c).

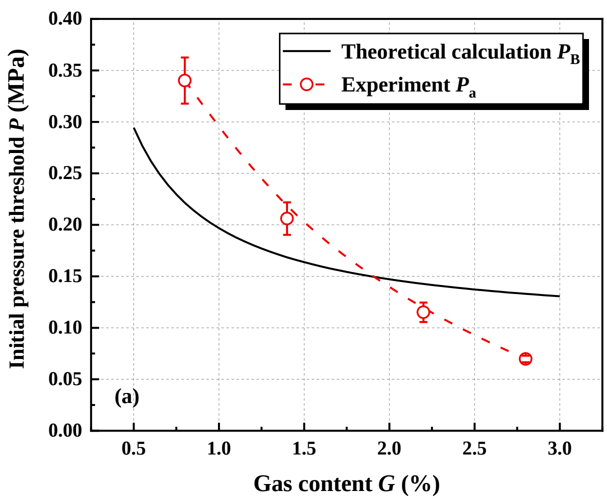

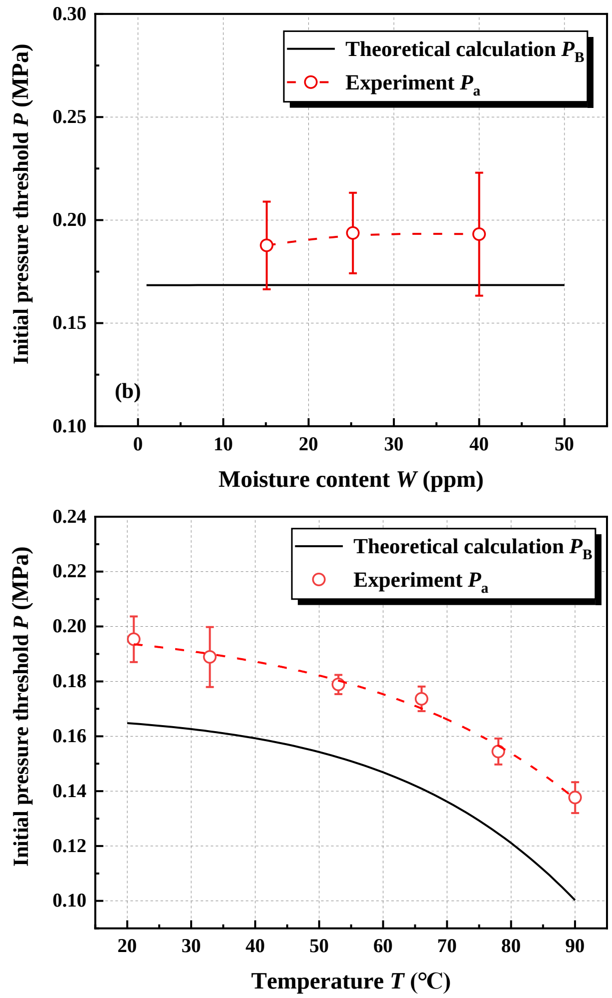

FIGURE 13 Relationship among initial pressure threshold and gas content, water content, and temperature of transformer oil. (a) W=14.9 ppm, T=25 ℃. (b) G=1.4 %, T=25 ℃. (c) W=14.9 ppm, G=1.4 %. P_B is the theoretical calculation result according to Eqs. (10)-(13). P_a is the experimental result according to Figure 11(b).

To conclude, the vibration-induced cavitation process is the key to the bubble initiation at the oil gap. Threshold characteristics of the bubble initiation process are determined by the initial radius and numbers of the bubble nucleus, the surface tension coefficient of transformer oil, and water saturation vapor, which are the key parameters affected by gas content, moisture content, and temperature of the oil.

5 CONCLUSIONS

This study centered on the characteristics and mechanism of bubble initiation at the transformer oil gap under vibration. The conclusions can be summarized as follows.

1. A significant bubbling phenomenon can be observed at the oil gap under vibration. Typical bubble structures, such as radiant bubble clouds and bubble flows, are further observed when the gap expands. The bubble initiation process has a significant threshold characteristic.
2. Factors affecting the threshold characteristics of the bubble initiation process are experimentally obtained. Bubbles at the oil gap under vibration are easier to initiate by increasing gas content, enhancing temperature, and decreasing moisture content. Vibrational frequency does not affect the threshold characteristics of the bubble initiation process.
3. The essence of bubble initiation is the decrease in pressure at the oil gap caused by the vibration-induced cavitation process. Threshold characteristics of the bubble initiation process are determined by the initial radius and number of the bubble nucleus, the surface tension coefficient of transformer oil, and water saturation vapor, which are the key parameters affected by gas content, moisture content, and temperature of the oil.

This work contributes to understanding the characteristics and mechanism of bubble initiation in oil-paper insulation systems, and may also provide a reference for risk assessment of abnormal vibration of oil-immersed power transformers and high-voltage reactors.

ACKNOWLEDGMENT

This study was financially supported by the Technology Project of State Grid Anhui Electric Power Company (contract number: 52120520001A).

CONFLICT OF INTEREST STATEMENT

The authors have no conflict whether in the research field or to publish the paper "Characteristics and Mechanism of Bubble Initiation in Transformer Oil Induced by Vibration" on "IET Generation, Transmission & Distribution".

DATA AVAILABILITY STATEMENT

The data that support the findings of this study are available from the corresponding author upon reasonable request.

REFERENCES

1. Borucki, S.: Diagnosis of technical condition of power transformers based on the analysis of vibroacoustic signals measured in transient operating conditions. IEEE Trans. Power. Del. 27(2), 670-676 (2012)
2. Shi, Y., Ji, S., Zhang, F.: Multi-frequency acoustic signal under short-circuit transient and its application on the condition monitoring of transformer winding. IEEE Trans. Power. Del. 34(4), 1666-1673 (2019)
3. Zhang, F., Ji, S., Shi, Y.: Research on transformer winding vibration and propagation characteristics. Proc. CSEE. 38(9), 2790-2798 (2018)
4. Hill, J. P., Wang, Z., Liu, Q.: Improvements to the construction of bubble inception formulae for use with transformer insulation. IEEE Access. 7, 171673-171683 (2019)
5. Yang, C., Zhao, T., Liu, Y.: Prediction model of bubble formation in oil-paper insulation based on the ITBE envelope. IEEE Trans. Dielectr. Electr. Insul. 29(5), 1735-1744 (2022)
6. Zhang, R., Zhang, Q., Guo, C.: Effects of thermally induced bubbles on the discharge characteristics of oil-impregnated pressboard. IEEE Trans. Dielectr. Electr. Insul. 29(3), 1191-1199 (2022)
7. Ben, T., Yang, Q., Yan, R.: Stress analysis of magnetically controlled reactor. AIP Adv. 7(5), 1-5 (2017)
8. Gao, M., Zhang, Q., Ding, Y.: Investigation on bubbling phenomenon in oil-paper insulation. IEEE Trans. Dielectr. Electr. Insul. 24(4), 2362-2370 (2017)
9. Zhang, R., Zhang, Q., Guo, C.: Bubbles in transformer oil: Dynamic behavior, internal discharge, and triggered liquid breakdown. IEEE Trans.

Dielectr. Electr. Insul. 29(1), 86-94 (2022)
10. Zhang, R., Zhang, Q., Zhou, J.: Partial discharge characteristics and deterioration mechanisms of bubble-containing oil-impregnated paper. IEEE Trans. Dielectr. Electr. Insul. 29(4), 1282-1289 (2022)
11. Brennen, C. E.: Cavitation and bubble dynamics. Oxford University Press, Oxford (1995)
12. Yasui, K.: Acoustic cavitation and bubble dynamics. Springer Nature Press, Japan (2018)
13. Guo, C., Zhang, Q., Zhang, R.: Investigation on gas generation characteristics in transformer oil under vibration. IET Gener. Transm. Distrib. 16, 5026-5040 (2022)
14. Heinrichs, F. W.: Bubble formation in power transformer windings at overload temperatures. IEEE Transactions on Power Systems. 98(5), 1576-1582 (1979)
15. Korobeynikov, S. M., Bychkov, A. Y., Ryzhkina, A, Y.: Microbubbling in transformer oil due to vibration. IEEE Trans. Dielectr. Electr. Insul. 20(2), 675-677 (2013)
16. Korobeynikov, S. M., Bychkov, A. L., Ridel, A. V.: Gassing in transformer oil at low and high frequency vibration. In: 11th International Forum on Strategic Technology (IFOST). 405-407. Novosibirsk (2016)
17. Kaufman, G., McMillen, C.: Gas bubble studies and impulse tests on distribution transformers during loading above nameplate rating. IEEE Trans. Power Apparat. Syst. 102(8), 2531-2542 (1983)
18. Liu, Y., Chao, N., Zhao, T.: Mechanism and numerical model of bubble effect in oil-paper insulation based on microtubule model. IEEE Trans. Dielectr. Electr. Insul. 27(5), 1529-1537 (2020)
19. IEC International Standard 60641-2. Pressboard and press paper for electrical purpose-part 2: methods of tests. International Electrotechnical Commission (IEC), Geneva, Switzerland (2007)
20. Wei, X., Wu, S., Jiang, N.: Theoretical and experimental analyses on high-voltage reactor vibration characteristics. High Volt. Apparat. 55(11), 66-73 (2019)
21. Wu, S., Ji, S, Sun, J.: Vibration monitoring and variation law of converter transformer in operation. High Volt. Eng. 48(4), 1561-1570 (2022)
22. Emsley, A. M., Xiao, X., Heywood, R. J.: Degradation of cellulosic insulation in power transformers. Part 3: Effects of oxygen and water on aging in oil. IEEE Proc. Sci. Measur. Techn. 147(3), 115-119 (2000)
23. Emsley, A. M., Stevens, G. C.: Review of chemical indicators of degradation of cellulosic electrical paper insulation in oil-filled transformer. IEEE Proc. Sci. Meas. Technol. 141(5), 324-334 (1994)
24. Przybylek, P., Moranda, H., Walczak, K.: The bubble effect in bushings-investigations on models. IEEE Trans. Dielectr. Electr. Insul. 22(6), 3405-3412 (2015)
25. Oommen, T. V., Lindgren, S. R.: Bubble evolution from transformer overload. IEEE/Pes Transmission and Distribution Conference and Exposition, Atlanta, GA, USA, 137-142 (2001)
26. He, X.: Study on bubble formation characteristics of oil paper insulation under vibration and temperature. M. S. thesis, Xi'an Jiaotong University, Xi'an, China (2021)
27. Chen, B., Wu, H.-y., Zhang, X.-m.: Detection on interfacial tension of insulating oil with trace water based on mid-infrared spectroscopy. Opt. Precis. Eng. 23(9), 2452-2458 (2015)